

Supplementary information

Immunosensor towards Low-Cost, Rapid Diagnosis of Tuberculosis

Jong-Hoon Kim,^{1,†} Woon-Hong Yeo¹, Zhiquan Shu,¹ Scott D. Soelberg,² Shinnoske Inoue,¹ Dinesh Kalyanasundaram,¹ John Ludwig,¹ Clement E. Furlong,² James Riley,¹ Kris Weigel,³ Gerard A. Cangelosi,³ Kieseok Oh,⁴ Kyong-Hoon Lee,^{4*} Dayong Gao,^{1*} and Jae-Hyun Chung^{1*}

¹Department of Mechanical Engineering, University of Washington, Box 352600, Seattle, Washington 98195

²Departments of Medicine-Division of Medical Genetics and Genome Sciences, University of Washington, Seattle, WA 98195

³Seattle Biomedical Research Institute, 307 Westlake Ave N, Suite 500, Seattle, WA 98109

⁴NanoFactory, Inc., P.O. Box 52651, Bellevue, WA 98015

*e-mail : jae71@uw.edu

Contents

1. Fabrication procedure of microtips
2. Microtip functionalization
3. Analysis for streaming flow
4. Electrohydrodynamic (EHD) flow and dielectrophoresis
5. Optimization of the concentration method
6. ELISA test for Anti-BCG IgY
7. Characterization of processed sputum samples

1. Fabrication procedure of microtips

Microtips were fabricated in a microfabrication laboratory (Washington Technology Center, University of Washington) as illustrated in Fig. S1(a). The microtips were fabricated from Si wafers with a diameter of 100mm. Using low pressure chemical vapor deposition (LPCVD), a 1 μm -thick silicon nitride layer was grown on Si wafers (100 mm in diameter). Rectangular areas were patterned on the back side of the Si_3N_4 layer using conventional UV lithography and etched using reactive ion etching (RIE) followed by KOH etching. The wavy-shape of the tip was then patterned on the Si_3N_4 layer and etched by the RIE process to create free-standing microtips. Finally, the tip surface was coated with gold for electrical conductivity. Fig. S1(b) shows microtip images by scanning electron microscopy (SEM, NanoTech User Facility, University of Washington).

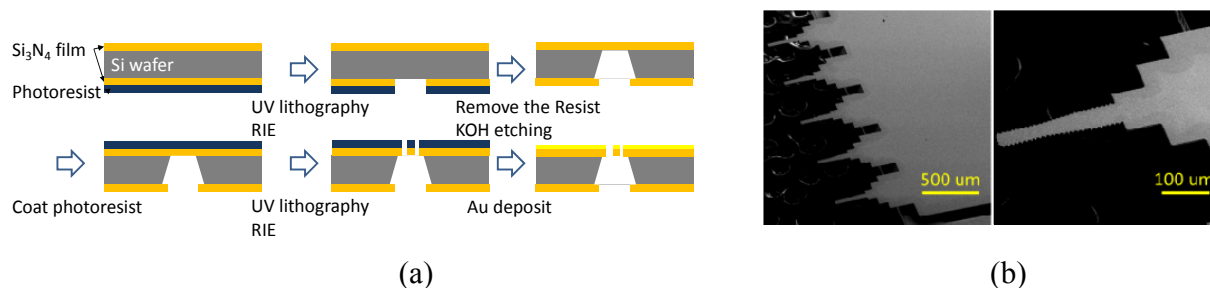


Figure S1. (a) Microtip fabrication procedure. (b) SEM images of the microtips.

2. Microtip functionalization

Microtip functionalization (Fig. S2) began with a coating of polyethyleneimine (1% PEI in DI water, Sigma-Aldrich) as an adhesive layer. The PEI treated tip was then immersed in biotinylated bovine serum albumin (10mg/mL BSA in PBS, Sigma-Aldrich) for 5 minutes. The biotin-BSA coated tip was coupled with streptavidin (1mg/mL in PBS, Sigma-Aldrich) for 1 minute. For the specific binding, the streptavidin-coated tip was coated with the biotinylated IgY antibodies (3 mg/ml in PBS).

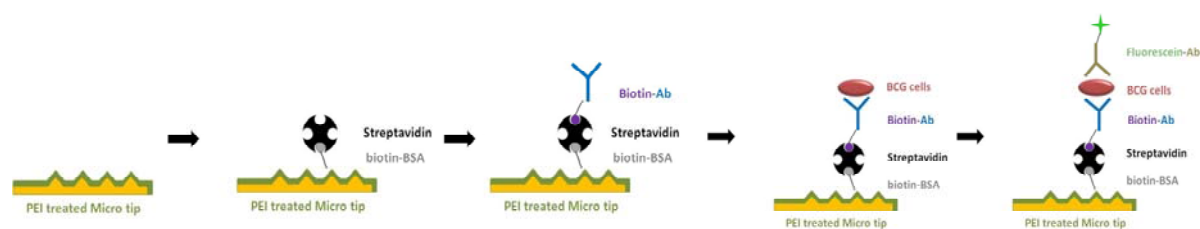


Figure S2. Functionalization process of a microtip

3. Analysis for streaming flow

The fluid motion was analyzed by tracing 19.0 μm -diameter polystyrene spheres in the steady state of the flow. Particle image velocimetry (PIV) analysis showed that 3 dimensional circulation flow delivered particles to the center of the well. The flows were measured for 2 horizontal-, 3 vertical-, and 3 side planes [Fig. S3(a)], which were integrated into 3 dimensional flow as shown in Fig. S3(b). Microtips were immersed in the center of the well where the flow velocity was reduced to 100 $\mu\text{m}/\text{second}$. Thus target particles were delivered to microtips by the circulation flows.

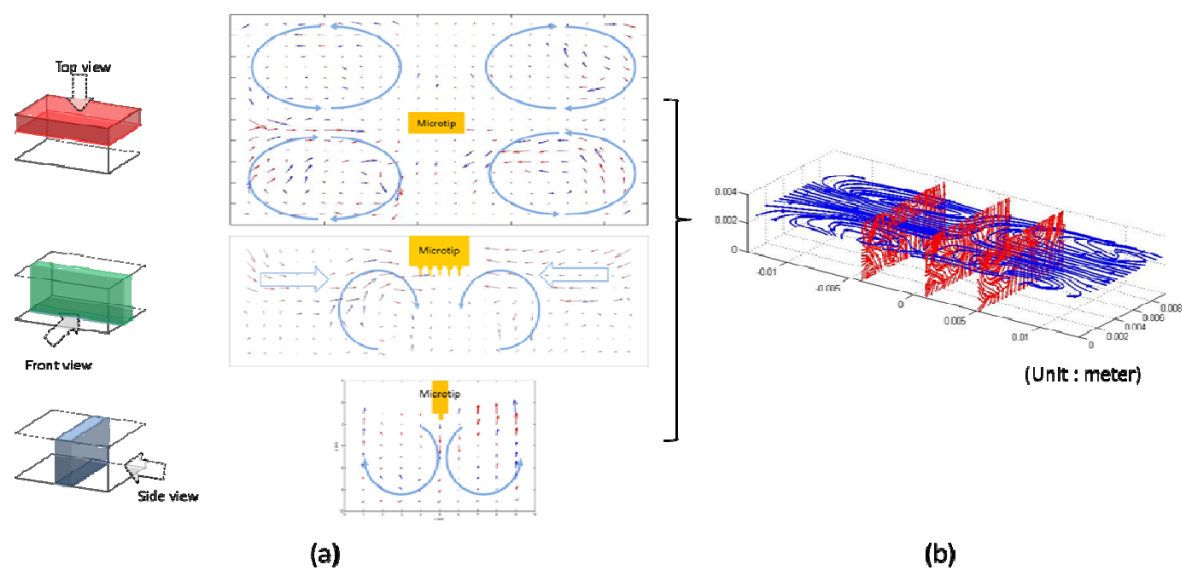


Figure S3. (a) PIV analysis of 2 dimensional flow for each plane, which is generated by longitudinal vibration of an aluminum well. (b) 3 dimensional flow that is generated by combining 2 dimensional flows.

4. Electrohydrodynamic (EHD) flow and dielectrophoresis

EHD flow can be generated by electroosmotic- and electrothermal flows. To clarify the generation mechanism of EHD flow, the flow velocities were measured according to frequency variation. The change of the flow velocities was also compared with the trend presented by analytical equations for electroosmotic- and electrothermal flows.

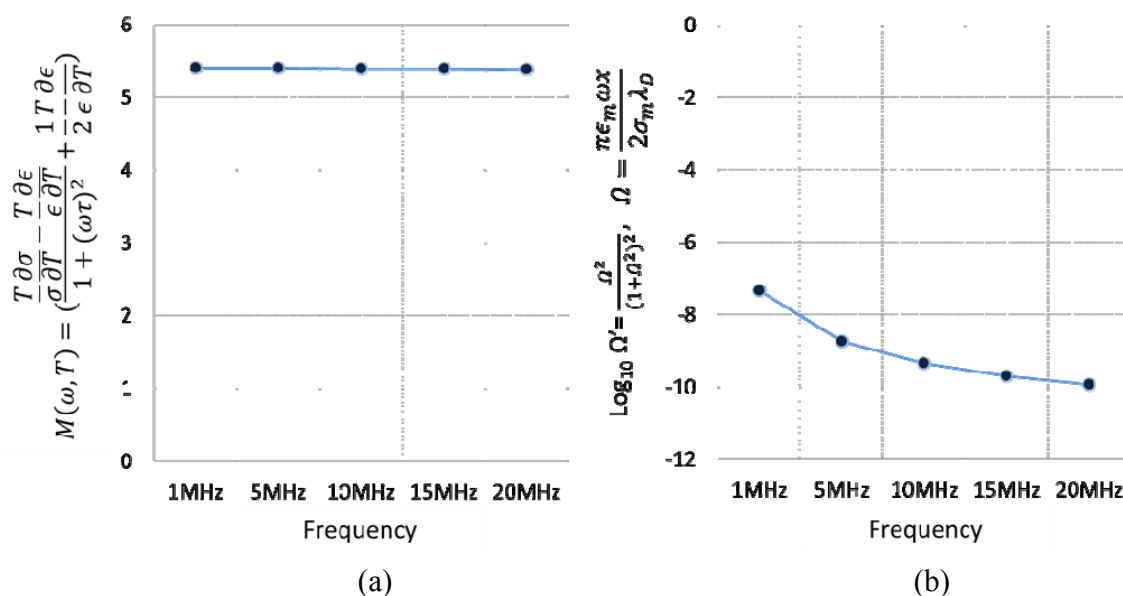


Figure S4 Factors proportional to velocities of electrothermal- and electroosmotic flows in terms of frequency variation (a) M factor for electrothermal flow (b) $\frac{\Omega^2}{(1 + \Omega^2)^2}$ for electroosmotic flow. This parameter is the dominant variable of time-averaged AC electroosmotic velocity.

Electrothermal flow arises from the temperature gradient in a medium generated by joule heating of the fluid. This temperature gradient induces local changes in the conductivity, permittivity, viscosity, and density of the solution. These gradients can generate forces acting on fluid. An electrothermal factor M (Ramos et al.) is given by:

$$M(\omega, T) = \left(\frac{T \partial \sigma}{\sigma \partial T} - \frac{T \partial \epsilon}{\epsilon \partial T} + \frac{1 T \partial \epsilon}{2 \epsilon \partial T} \right) \frac{1}{1 + (\omega \tau)^2} \quad (S1)$$

$M(\omega, T)$ is a dimensionless factor that shows the variation of the electrothermal force as a function of the frequency. Since the electrothermal force is proportional to the velocity of electrothermal flow, M factor is proportional to the velocity of electrothermal flow. The value of $M(\omega, T)$ is calculated for $\sigma=1.58$ S/m, $T=300$ K, $\varepsilon=80\varepsilon_0$, $V=20$ V (peak to peak), $\omega=2\pi f$, and $\tau=\varepsilon/\sigma$. The computed M -values are shown in Fig. S4 (a). According to this analytical result, the flow velocity for electrothermal flow should be constant in the frequency range of 1~20MHz.

Time-averaged ac electroosmotic velocity is derived from a generalization of the Smoluchowski formula given by:

$$u_{ACEO} = A \frac{\varepsilon_m V_p^2}{8\mu\tau} \frac{\Omega^2}{(1+\Omega^2)^2}, \quad (\text{S2})$$

Here a nondimensional frequency Ω (Burg et al.) is:

$$\Omega = \frac{\pi \varepsilon_m \omega x}{2 \sigma_m \lambda_D}. \quad (\text{S3})$$

The value of Ω is calculated for $\varepsilon=80\varepsilon_0$, $\sigma=1.58$ S/m, $\lambda_D=1$ nm (double layer characteristic thickness), and $x=1$ mm (characteristic length in system). Fig. S4 (b) shows $\Omega' = \frac{\Omega^2}{(1+\Omega^2)^2}$ that continuously decreases between 1 and 20 MHz, meaning that the time-averaged AC electroosmotic velocity also decreases in the range.

In our experimental setup, Au-coated microtips without antibodies were used to observe the behavior of BCG cells under e-field. BCG cells at 10^7 CFU/mL in PBS buffer were stained with live-dead staining kits (LIVE/DEAD® BacLight™ Bacterial Viability Kit, Invitrogen). With an AC field, the circulation flows were generated with attraction of MTB cells on to microtip surface. The attraction process was video-recorded, which was analyzed by using mPIV (Matlab Particle Image Velocimetry) [Fig. S5(a)]. When the frequencies were changed from 1 MHz to 20 MHz, the EHD flow velocity was reduced from 456 $\mu\text{m/s}$ to 63 $\mu\text{m/s}$ in Fig. S5(b).

When the experimental results are compared with the analytical results for the frequency range of 1 ~ 20MHz, the drop of the flow velocity is consistent with the trend of Ω' for electroosmotic flow. If the flow is dominated by electrothermal flow, the flow velocity should be constant in the frequency range of 1MHz ~ 20MHz, following the trend presented in Fig. S4 (a). Thus the fluid flow at 5 MHz can be dominated by AC electroosmosis. When the frequency is greater than 10MHz, a flow velocity appears to reach a bottom plateau. This flow can be caused by electrothermal flow. According to the results, electroosmotic flow appears dominant at 5 MHz but electrothermal flow also coexists. The transition between electroosmotic- and electrothermal flows for 1.58 S/m buffer at 5 MHz is consistent with the previous analysis^{S1}. The delivered cells by EHD flow were attached to microtip surfaces by dielectrophoresis.

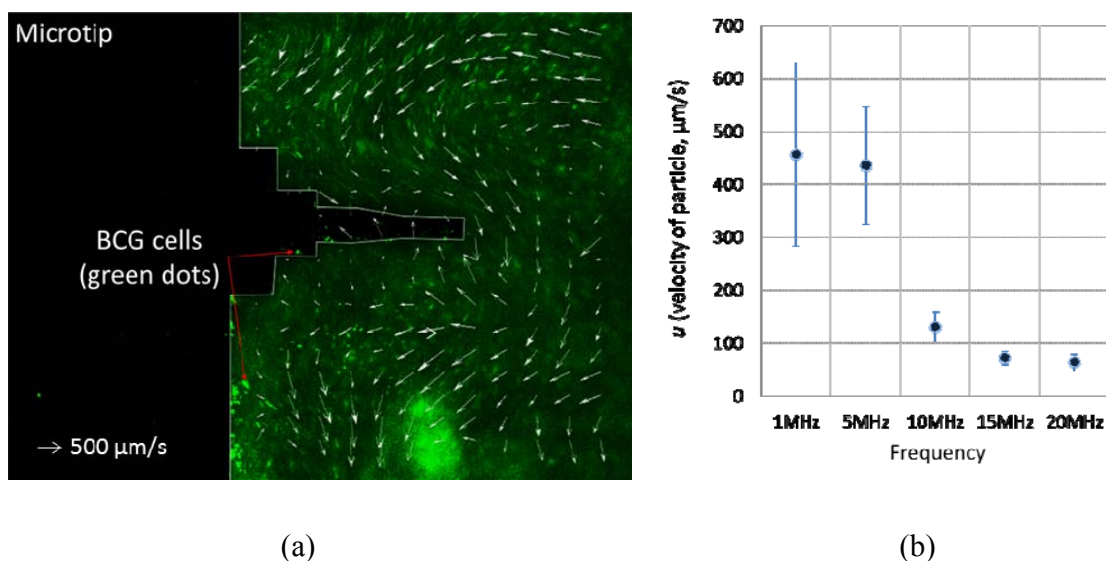


Figure S5. Motion of BCG cells under an AC e-field (5MHz at 20 V_{pp}). (a) Stained BCG cells were circulated around the microtip due to EHD flow and attracted on the surface of a microtip by DEP. (b) Average velocities of EHD flow in the vicinity of a microtip according to frequencies.

5. Optimization of the concentration method

Streaming flow, an electric field, its frequency, and tip withdrawal rate were optimized to improve the efficiency of concentration. (1) Streaming flow was optimized to achieve circulation flow that delivered target cells to microtips. To minimize aerosolization, the vibration motor was tuned to avoid excessive flow velocity. In repeated tests, uniform flow pattern was generated in the longitudinal vibration of an aluminum well at an amplitude of $45\mu\text{m}$ of 31.3 Hz. (2) For an electric field, 20Vpp was chosen because it was the maximum applicable voltage that did not damage the microtip surface. (3) 5MHz was chosen because the frequency below 1MHz could contaminate microtips in sputum samples. The contamination could happen by electrostatic attraction of unwanted particles on microtip surfaces in sputum. The frequency over 10 MHz was not used because EHD flow became negligible. (4) The withdrawal rate of microtips can be an important parameter to control the capillary action on the microtip surface. Using a linear motor, the withdrawal rates of $10\mu\text{m/s}$ and $100\mu\text{m/s}$ were tested but noticeable difference was not observed for the capturing performance. Thus a higher rate of $100\mu\text{m/s}$ was chosen to accelerate the concentration process.

6. ELISA test for Anti-BCG IgY

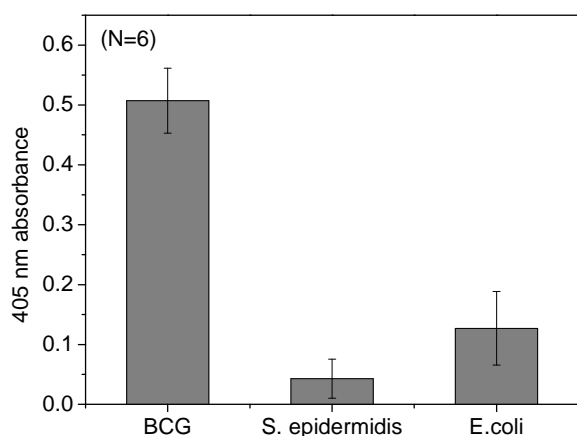


Figure S6. Anti-BCG IgY ELISA result.

Equal concentrations (OD 600 matched) of three different bacteria (BCG, *E. coli* and *S. epidermidis*, approximately 10^5 cells in 100 μ l PBS) were assayed for binding to anti-BCG IgY antibody using a 0.45 micron filter plate (Millipore #MAHVN4510) (Fig. S6). Aliquots of the bacterial suspensions were added to the 96-well filter bottom plate and washed with PBS (4x200 μ L). A 100 μ l aliquot of 10 μ g/ml IgY-BCG antibody in PBS was then added to the washed cells and incubated for 1 hour at 37C. After a PBS wash (4x200 μ l) a secondary antibody was added (rabbit anti-IgY-HRP conjugate, Thermo Scientific #31401) and incubated for 1 hour at 37C. The sample was then washed with PBS (4x200 μ l), followed by addition of 100ul ABTS substrate (Thermo Scientific #37615), incubated for 5 minutes, and filtered into 96-well receiver plate. Absorbance was then read at 405 nm.

7. Characterization of processed sputum samples

The sputum samples varied in terms of viscosity, opacity, and color. Conductivity and viscosity could be key parameters with regard to effective fluid motion. However, measurement tools for conductivity and viscosity require large sample volumes (>10 mL) and can be contaminated by sputum samples. Thus direct measurements of conductivity and viscosity were not conducted.

To estimate the conductivity of sample solution, a dominant reagent having the highest conductivity was studied. The conductivities of reagents for using sputum liquefaction were 1.58 S/m, 0.12 S/m, and 0.37 S/m for 1xPBS, 4mg/mL NALC, and 4% SDS, respectively. The conductivity of the mixture was 0.71 S/m, which was dominated by that of PBS.

Viscosity could not be measured due to contamination of a rheometer. To assess the variation of the processed sputum samples, turbidity using UV spectrophotometer was measured as the difference between the absorbance of the sample solution and a reference at the wavelength of

600nm. 6 sputum samples were randomly chosen and then processed following the liquefaction procedure. The processed sample was transferred to a cuvette, and the absorbance was measured at 600 nm using UV spectrophotometer (BioRad SmartSpec™ 3000). For the reference measurement, the mixture of PBS, NALC and SDS without sputum was used. The turbidity of the processed sputum samples was ranged from 0.027 to 0.118 at 600 nm while that of the original sputum was greater than 1. The measured turbidity values are shown in Table S1.

Table S1. Turbidity value at 600nm for 6 sputum samples

	1	2	3	4	5	6	Mean	SD
Turbidity	0.118	0.034	0.034	0.065	0.027	0.047	0.054	0.034

References:

S1. S. Park, M. Koklu and A. Beskok, *Anal. Chem.*, 2009, **81**, 2303–2310.